NASA TECHNICAL NOTE

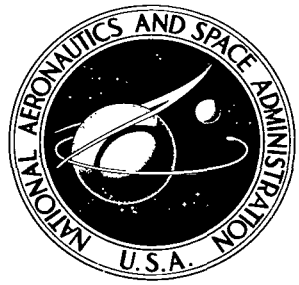

NASA TN D-8461

SUSCEPTIBILITY TO HOT CORROSION OF FOUR NICKEL-BASE SUPERALLOYS, NASA-TRW VIA, B-1900, 713C, and IN-738

Carl A. Stearns, Fred J. Kohl, and George C. Fryburg

Lewis Research Center
Cleveland, Ohio 44135

NATIONAL AERONAUTICS AND SPACE ADMINISTRATION • WASHINGTON, D. C. • APRIL 1977

1. Report No.	2. Government Accession No.	3. Recipient's Catalog No.
NASA TN D-8461		

4. Title and Subtitle: SUSCEPTIBILITY TO HOT CORROSION OF FOUR NICKEL-BASE SUPERALLOYS, NASA-TRW VIA, B-1900, 713C, AND IN-738

5. Report Date: April 1977

6. Performing Organization Code:

7. Author(s): Carl A. Stearns, Fred J. Kohl, and George C. Fryburg

8. Performing Organization Report No.: E-8977

9. Performing Organization Name and Address:
Lewis Research Center
National Aeronautics and Space Administration
Cleveland, Ohio 44135

10. Work Unit No.: 506-16

11. Contract or Grant No.:

12. Sponsoring Agency Name and Address:
National Aeronautics and Space Administration
Washington, D. C. 20546

13. Type of Report and Period Covered: Technical Note

14. Sponsoring Agency Code:

15. Supplementary Notes:

16. Abstract

The susceptibility to hot corrosion of four nickel-base, cast superalloys has been studied at 900° and 1000° C. The test consisted of coating alloy samples with known amounts of Na_2SO_4 and oxidizing the coated samples isothermally in 1 atmosphere of slowly flowing oxygen, the weight-gain being monitored on a sensitive recording microbalance. Two doses of Na_2SO_4 were used: 2/3 and 3 mg cm^{-2} Susceptibility to hot corrosion decreased in the order of decreasing molybdenum content of the alloys; namely, B-1900 > 713C > NASA-TRW VIA > IN-738. Preoxidation of samples before hot-corrosion testing markedly increased the induction period observed prior to the inception of hot corrosion for all alloys tested. X-ray diffraction analyses of the oxide scales were made. All samples that underwent hot corrosion showed the presence of a $(Ni, Co)MoO_4$ layer near the alloy-oxide interface. Several specimens of NASA-TRW VIA and one of IN-738 displayed resistance to hot corrosion and these showed $NaTaO_3$ as a prominent feature in their oxide scale. Our results may be interpreted as indicating that molybdenum in an alloy is detrimental, with respect to hot corrosion, while tantalum is beneficial.

17. Key Words (Suggested by Author(s))	18. Distribution Statement
Oxidation; Heat-resistant alloys; Chromium oxides; Aluminum oxides; Thermogravimetry; Corrosion	Unclassified - unlimited STAR Category 26

19. Security Classif. (of this report)	20. Security Classif. (of this page)	21. No. of Pages	22. Price*
Unclassified	Unclassified	18	A02

* For sale by the National Technical Information Service, Springfield, Virginia 22161

SUSCEPTIBILITY TO HOT CORROSION OF FOUR NICKEL-BASE SUPERALLOYS, NASA-TRW VIA, B-1900, 713C, AND IN-738

by Carl A. Stearns, Fred J. Kohl, and George C. Fryburg

Lewis Research Center

SUMMARY

The susceptibility to hot corrosion of four nickel-base, cast superalloys has been studied at 900° and 1000° C. The test consisted of coating alloy samples with known amounts of sodium sulfate and oxidizing the coated samples isothermally in 1 atmosphere of slowly flowing oxygen, the weight-gain being monitored on a sensitive recording microbalance. Two doses of sodium sulfate were used: 2/3 and 3 milligrams per square centimeter. Susceptibility to hot corrosion decreased in the order of decreasing molybdenum content of the alloys; namely, B-1900 > 713C > NASA-TRW VIA > IN-738. Preoxidation of samples before hot corrosion testing markedly increased the induction period observed prior to the inception of hot corrosion for all alloys tested. X-ray diffraction analyses of the oxide scales were made. All samples that underwent hot corrosion showed the presence of a $(Ni, Co)MoO_4$ layer near the alloy-oxide interface. Several specimens of NASA-TRW VIA and one of IN-738 displayed resistance to hot corrosion and these showed $NaTaO_3$ as a prominent feature in their oxide scale. Our results may be interpreted as indicating that molybdenum in an alloy is detrimental, with respect to hot corrosion, while tantalum is beneficial.

INTRODUCTION

The continually increasing performance demanded from gas-turbine engines requires ever increasing operating temperatures which, in turn, requires alloys with increased high-temperature strength and corrosion resistance. Higher strength has been achieved in the nickel-base alloys used in turbine blades by increasing the amounts of γ'-forming elements (Al and Ti) and of the solution strengthening elements (Mo, W, and Cr). This pursuit of high-temperature strength has been accompanied by a lowering of the chromium content of these alloys while increasing the aluminum content. This

trend has provided alloys with good oxidation resistance but with decreased resistance to hot corrosion. Hot corrosion is an accelerated, often catastrophic, attack experienced by superalloys that appears to be initiated by the deposition of condensed sodium sulfate (Na_2SO_4) on engine parts (ref. 1). The source of the salt is direct ingestion with intake air or its formation during combustion from sodium chloride contaminated air and sulfur in the fuel. The observation of hot corrosion has been occurring with increasing frequency in recent years and is expected to become more prevalent with the advent of the newer turbine engines with higher compression ratios. Thus, it is anticipated that hot corrosion will become the major barrier to the increase in use-temperature of alloy systems for the gas turbine engine.

Most superalloys are susceptible to hot-corrosion attack to some extent, and the phenomenon is known to depend on many factors, which include temperature, cyclic conditions, composition of alloy, impurities in and pressure of air ingested into the engine, and impurities in the fuel burned by the engine. Because of the complexity of the problem, research has been concerned mainly with phenomenological testing of alloys. Research directed toward an understanding of the reaction mechanisms has been less prevalent[1] and, as a result, a complete fundamental characterization of hot corrosion is lacking.

As part of a larger program aimed at understanding the chemical mechanisms involved in hot-corrosion, we have conducted a laboratory test study involving thermogravimetric rate determinations of the induced hot corrosion of four superalloys, NASA-TRW VIA, B-1900, alloy 713C, and IN-738. The object of the investigation was twofold: to develop a short laboratory test to measure the rate of hot corrosion in a reproducible, quantitative manner that could be used to test various hot-corrosion agents and to determine the relative susceptibility to hot corrosion of four representative nickel-base superalloys.

A previous report (ref. 4) presented the straight oxidation behavior of these four alloys. Tests were conducted at 900° and 1000° C in slowly flowing oxygen. Oxidation rates were given as well as descriptions of morphology and composition of oxide scales formed after 100 hours at temperature. This report will be referred to as paper I.

EXPERIMENTAL

The alloy samples were obtained from commercial sources and were given conventional heat treatments as described in paper I. The chemical compositions are repeated in table I and are given in atomic percent as well as weight percent.

[1]Exceptions to this trend have been the work of Goebel, Petit, and Goward (ref. 2) and Bornstein, DeCrescente, and Roth (ref. 3).

The samples were identical in size to those used in paper I (0.2 by 1.0 by 2.5 cm) with a hangdown hole in one end. The surfaces were glass-bead blasted to give a uniform matte surface and were cleaned ultrasonically in chloroform and in detergent, and rinsed with water, acetone, and ethanol.

Specimens were subjected to isothermal Na_2SO_4-induced oxidations; that is, hot corrosion tests. The specimens were sprayed with a saturated solution of reagent grade Na_2SO_4 in distilled water just before starting the hot corrosion test. The spraying technique was similar to that described by Bornstein and DeCrescente (ref. 5) and consisted of heating the specimens on a hot plate at 200° C and spraying them with an air brush. The specimens were weighed before and after spraying in order to calculate the amount of salt coating. Coatings of 2/3 and 3 milligrams per square centimeter Na_2SO_4 were used.

Chemical analysis of the coatings indicated that little or no water of hydration was in the coatings. X-ray diffraction indicated the coatings were primarily thenardite, an anhydrous form of Na_2SO_4.

Tests were run at two temperatures, 900° and 1000° C, in slowly flowing oxygen at a pressure of 1 atmosphere. The direction of flow of oxygen was downward, and the speed was 20 centimeters per minute. Both unoxidized samples and samples that had been preoxidized for 100 hours at the test temperature were used. As in paper I, continuous gravimetric measurements were made using a Cahn R-100 microbalance. Samples were suspended by a platinum - 13-percent-rhodium chain into a temperature regulated tube furnace. The furnace was mounted on a vertical track to allow raising and lowering. The enclosure tube was 2.5-centimeter-outside-diameter quartz tubing. Corrections in the weight change were made for the effect of buoyancy. Exposure times extended in some cases to 450 hours.

Oxide scales were examined by X-ray diffraction using standard techniques.

RESULTS AND DISCUSSION

Thermogravimetric Rate Studies

Rate curves for a set of six B-1900 specimens corroded at 900° C with a 2/3-milligram-per-square-centimeter Na_2SO_4 dose are shown in figure 1 where we have plotted the specific weight gain against the time. Attempts were made to quantize the hot corrosion data by fitting them to a parabolic rate curve. However, the time interval over which the data could be fitted satisfactorily was of such short duration that the parabolic rate constants obtained displayed little correlation with the amount of corrosion that occurred.

The reproducibility of the data in figure 1 is roughly ±15 percent and is typical for specimens that were not preoxidized. Preoxidized samples displayed a more varied behavior, especially with regard to the length of the induction period. The induction period is not so obvious in figure 1 because of the relatively insensitive time scale. Nevertheless, the onset of hot corrosion in all four of the alloys tested here is preceded by an induction period; that is, a period of little or no weight gain. It is difficult to define quantitatively the length of the induction period. We have arbitrarily chosen the period of time required for the specimens to attain a specific weight gain of 0.3 milligram per square centimeter. The length of the induction period is dependent on the temperature, the alloy, the dose of Na_2SO_4, and the preoxidation treatment of the alloy. The induction period is generally followed by a period of rapidly accelerating weight gain that may either consume the entire sample (catastrophic oxidation) or transform into a period of decelerating weight gain, resulting in final cessation of oxidation (enhanced or accelerated oxidation).

A comparison between hot corrosion and simple oxidation is instructive. The B-1900 specimens illustrated in figure 1 have gained roughly 80 milligrams per square centimeter after 100 hours of oxidation, and appear as shown in figure 2 after cooling to room temperature. The unreacted alloy, about one half of the original, is in the center of the picture. The oxide scale on the edge has peeled off. The oxide on the side faces has peeled back intact but is held in place at the top by the platinum alloy hook. The appearance of this specimen is typical of specimens that underwent accelerated oxidation. In simple oxidation, B-1900 samples would have gained only 0.2 milligram per square centimeter in 100 hours (see paper I). We see that hot corrosion results in enhanced weight gains of hundreds of times and as such poses a serious threat to the integrity of aircraft engine components. Any component having undergone the amount of corrosion depicted in figure 2 would have failed. However, we must remember that these laboratory tests are deliberately accelerated for obvious reasons.

Comparative rate curves for the four alloys corroded at 900° C are given in figure 3. In figure 3(a) we compare the corrosion rates of samples given no preoxidation and coated with 2/3 milligrams per square centimeter of Na_2SO_4. All four alloys show enhanced oxidation and the order of decreasing susceptibility is B-1900 > 713C > VIA > 738. It may be noted that VIA and 738 exhibit plateau regions in their corrosion curves. Alloy 738 has not undergone as much corrosion as the other three alloys and appeared as shown in figure 4 after cooling to room temperature. Several specimens of VIA exhibited resistance to hot corrosion displaying weight gains of only 0.5 to 2 milligrams per square centimeter after 100 hours of Na_2SO_4 induced oxidation. Other specimens hot corroded on only a corner. X-ray diffraction analysis indicated the presence of different oxides in the scale. These results will be discussed in the section Analysis of Oxide Scales.

In figure 3(b) we compare the rates of samples that were preoxidized for 100 hours before being coated with 2/3 milligram per square centimeter of Na_2SO_4. As before, all alloys exhibit enhanced oxidation, and the extent of oxidation is roughly the same or somewhat less than for nonpreoxidized samples. The order of susceptibility is B-1900 > 713C > VIA > 738. The most striking feature of these results is the large increase in the induction period effected by the preoxidation: for B-1900 it has increased from 1/2 to 6 hours, for 713C from 2 to 22 hours, for VIA from 1 to 5 hours, and for 738 from 2 to 3 hours. The large increase in the induction period for preoxidized 713C prevents this alloy from hot corroding as rapidly as VIA, nevertheless, the extent of the corrosion after long exposures is greater than with VIA.

As stated previously, it is difficult to define quantitatively the length of the induction period. Our definition of the period of time required for the specimens to attain a specific weight gain of 0.3 milligram per square centimeter does not take into account the slope of the curve of weight gain against time, and it tends to detract from the importance of the long period of very little weight gain observed with 738 and preoxidized 713C.

In figure 3(c) we present the comparative data for samples given no preoxidation and treated with 3 milligrams per square centimeter of Na_2SO_4. All four alloys have undergone catastrophic oxidation and are completely consumed. It should be noted that 738 displays a long plateau region before the catastrophic corrosion begins, and in shorter tests it would be judged resistant to hot corrosion. However, the specimen was completely consumed, and on cooling to room temperature split down the center into two large oxide scales as shown in figure 5.

Corrosion rates for samples preoxidized for 100 hours at 900° C and treated with 3 milligrams per square centimeter are shown in figure 3(d). Three alloys, B-1900, 713C, and VIA exhibited catastrophic oxidation. The induction periods have been increased noticeably: for B-1900 from $2\frac{1}{2}$ to $7\frac{1}{2}$ hours, for 713C from $2\frac{1}{2}$ to 7 hours, and for VIA from 2 to $7\frac{1}{2}$ hours. Alloy 738 seemed to be resistant to corrosion for a period out to 460 hours and appeared as shown in figure 6. It is difficult to assess whether this behavior is a result of an extended induction period or of a real resistance. In both figures 3(c) and (d) we again observe the same order of susceptibility to hot corrosion: B-1900 > 713C > VIA > 738.

Comparative rate curves for the four alloys corroded at 1000° C are given in figure 7 for the low and high doses of Na_2SO_4. These data are for nonpreoxidized samples. With the low dose Na_2SO_4 (fig. 7(a)) the four alloys show enhanced oxidation. The rates are increased over the rates at 900° C (fig. 3(a)) especially for 738, which has undergone extensive corrosion at 1000° C. With the high dose Na_2SO_4 (fig. 7(b)) all four alloys display catastrophic oxidation, and the rates have increased noticeably over the rates at 900° C (fig. 3(c)). A typical specimen that has undergone catastrophic oxidation is shown in figure 8. Only a thin section of unreacted alloy remains at the top, and

the sample consists of four large oxide leaves. The order of decreasing susceptibility to hot corrosion for these results is not quite as well defined as at 900° C, but it appears to be essentially the same.

Rate curves for preoxidized samples have not been included in these higher temperature results. At 1000° C the induction period is a much less important feature of the hot-corrosion curve. For unoxidized specimens it is only 10 to 15 minutes for these four alloys. Preoxidation at 1000° C for 100 hours may increase the induction period to 1 to 2 hours only, after which corrosion proceeds in a parallel fashion but displaced in time. This behavior is depicted in figure 9 for B-1900 on an expanded time scale.

X-Ray Diffraction Analysis of Oxide Scales

The oxide scales formed on the specimens during induced oxidation were generally very thick and peeled off on cooling to room temperature (as shown in figs. 2, 5, and 8). The peeled oxides were very porous and were colored pale green with a dense black outer surface. X-ray diffraction analyses were made of the oxide that remained on the specimens, of the outside and underside of thick scales that remained intact after peeling from the sample, and of samples made by grinding up some of the intact scales.

The oxide phases identified on the specimens for different temperatures and Na_2SO_4 doses are presented in table II, and those identified in the oxide scales are presented in table III. The phases are listed in order of the decreasing intensity of their diffraction patterns, although this is not necessarily related to their relative quantity on the sample. Generally, there was no difference between hot-corrosion produced oxides formed on specimens that had been preoxidized and those that had not been. Therefore, this distinction has not been included in the tables II and III.

The most prominent feature of the data of table II is the occurrence of nickel molybdate ($NiMoO_4$) on every specimen. The $NiMoO_4$ was especially prominent on B-1900, which contains the highest percentage of molybdenum. It is believed that the $NiMoO_4$ contained a considerable fraction of cobalt,[2] as the diffraction pattern for $CoMoO_4$ is very similar to that for $NiMoO_4$. The intensity of the $NiMoO_4$ pattern in the peeled oxides was usually much less than that from the oxide retained on the sample, which indicates that the oxide peeled off just above a $NiMoO_4$ layer that was close to the alloy-oxide interface. Brenner (ref. 6) has shown that $NiMoO_4$ undergoes allotropic phase transformations on cooling so that a $NiMoO_4$ layer would constitute a region of weakness in the oxide scale.

Spinels are present in the oxide retained on the samples. On B-1900 and VIA, the spinel is a mixed aluminum-chromium spinel with $a_o = 8.15 \times 10^{-10}$ m. The a_o value

[2]Except for alloy 713C, which contains no cobalt.

increases in the oxide on 713C to 8.2×10^{-10} m, and to 8.30×10^{-10} m on 738, as the chromium content of the alloy increases.

Tapiolite ($(Ni, Co)(Ta, Nb, Mo, W)_2O_6$) was observed in the retained oxide (see paper I for details). It was most prevalent on VIA, the alloy that contains the highest percentage of tantalum. On 738, titanium dioxide (TiO_2) was also observed as a distinct phase, as was chromium sesquioxide (Cr_2O_3). Nickel oxide (NiO) was observed in most retained oxides.

For the peeled oxides the most prominent feature was NiO. This was especially prominent in the black outside surface where it was the major constituent. The other prominent oxide in the peeled oxides was spinel that had the same a_o spacings as in the oxides retained on different alloys. In addition, tapiolite was observed in the oxides from VIA. No indications of any of the sulfides of chromium or nickel were detected in any of the scales.

In summary, the oxide scale formed during oxidation induced with Na_2SO_4 consists of an outer black surface of NiO, beneath which is a thick porous green oxide composed of a mixture of NiO and spinel. Below the porous oxide, near the oxide-alloy interface, is a layer of $(Ni, Co)MoO_4$. At the oxide-alloy interface is a thin layer, which is a complicated mixture of oxides, the nature of which depends on the composition of the alloy (see table I).

As mentioned in the previous section, several specimens of VIA exhibited resistance to Na_2SO_4 induced oxidation at 900° C. X-ray diffraction analysis of the oxide scale on these specimens detected a very strong pattern of $NaTaO_3$ in addition to strong spinel ($a_o = 8.15\times10^{-10}$ m), medium tapiolite, and weak NiO. Likewise, X-ray diffraction analysis of the oxide on the preoxidized 738 specimen that resisted hot corrosion for 460 hours (see fig. 3(d)) detected a strong pattern for $Na(Ta, Nb)O_3$ in addition to very strong NiO and medium spinel ($a_o = 8.30\times10^{-10}$ m). It appears, therefore, that tantalum may provide a beneficial effect in hot corrosion by combining with Na_2O, possibly by the reaction

$$Na_2SO_4 + Ta_2O_5 \rightarrow 2NaTaO_3 + SO_3$$

CONCLUDING REMARKS

Results of this study indicate that alloys can be ranked in order of their susceptibility to hot corrosion by a simple laboratory test. However, the ranking is only qualitative because of the complexity of the curve of specific weight gain against time.

All the alloys underwent hot corrosion under some conditions, and, once hot corrosion began, it proceeded rapidly to such an extent that the structural integrity of the

alloy was compromised. It appears that prevention of hot corrosion must be attained by the prevention of the initiation reactions of hot corrosion, those processes occurring during the induction period. An understanding of these processes leading up to the initiation of hot corrosion should indicate methods of prevention.

Our results also indicate that the presence of molybdenum in an alloy may be detrimental, with respect to hot corrosion, while tantalum may be beneficial.

Lewis Research Center,
National Aeronautics and Space Administration,
Cleveland, Ohio, December 9, 1976,
506-16.

REFERENCES

1. Stringer, J.: Hot Corrosion in Gas Turbines. MCIC-72-08, Battelle Columbus Labs. (AD-745474), 1972.

2. Goebel, J. A.; Pettit, F. S.; and Goward, G. W.: Mechanisms for the Hot Corrosion of Nickel-Base Alloys. Metall. Trans., vol. 4, no. 1, Jan. 1973, pp. 261-278.

3. Bornstein, N. S.; DeCrescente, M. A.; and Roth, H. A.: The Relationship between Relative Oxide Ion Content of Na_2SO_4, the Presence of Liquid Metal Oxides, and Sulfidation Attack. Metall. Trans., vol. 4, no. 8, Aug. 1973, pp. 1799-1810.

4. Fryburg, George C.; Kohl, Fred J.; and Stearns, Carl A.: Oxidation in Oxygen at 900° and 1000° C of Four Nickel-Base Cast Superalloys: NASA-TRW VIA, B-1900, Alloy 713C, and IN-738. NASA TN D-8388, 1977.

5. Bornstein, N. S.; and DeCresente, M. A.: The Role of Sodium in the Accelerated Oxidation Phenomenon Termed Sulfidation. Metall. Trans., vol. 2, no. 10, Oct. 1971, pp. 2875-2883.

6. Brenner, S. S.: Oxidation of Iron-Molybdenum and Nickel-Molybdenum Alloys. J. Electrochem. Soc., vol. 102, 1955, pp. 7-15.

TABLE I. - COMPOSITION OF SUPERALLOYS

Element	Alloy							
	B-1900		NASA-TRW VIA		Alloy 713C		IN-738	
	Composition							
	wt %	at. %	wt %	at. %	wt %	at. %	wt %	at. %
Nickel	64.5	62.5	62	64.5	72	67	61.5	59
Chromium	8.0	8.7	6.1	7.1	12.5	13.2	16.0	17.5
Aluminum	6.0	12.6	5.4	12.2	6.1	12.4	3.4	7.2
Titanium	1.0	1.2	1.0	1.3	.8	.9	3.4	4.0
Cobalt	10.0	9.6	7.5	7.7	------	-----	8.5	8.2
Molybdenum	6.0	3.5	2.0	1.3	4.2	2.4	1.7	1.0
Tungsten	[a].1	-----	5.5	1.8	------	-----	2.6	.8
Tantalum	4.3	1.4	9.0	3.0	------	-----	1.7	.6
Niobium	[a].1	-----	.5	.3	2.0	1.2	.9	.6
Hafnium	------	-----	.4	.1	------	-----	-----	-----
Zirconium	.08	-----	-----	----	------	-----	.1	.06
Rhenium	------	-----	.3	.1	------	-----	-----	-----
Iron	[a].35	-----	-----	-----	[a]2.5	[a]2.5	[a].5	-----
Carbon	.1	.47	.13	.66	.12	.55	.17	.81
Boron	.015	-----	-----	-----	[a].012	-----	.01	-----
Silicon	[a].25	-----	-----	-----	[a].5	-----	[a].3	-----
Manganese	[a].2	-----	-----	-----	[a].25	-----	[a].2	-----

[a]Maximum value.

TABLE II. - PHASES IDENTIFIED BY X-RAY DIFFRACTION IN OXIDES RETAINED ON SPECIMENS AFTER Na_2SO_4-INDUCED OXIDATION IN 1 ATMOSPHERE OF FLOWING OXYGEN

Alloy	Temperature, °C	Dosage of Na_2SO_4, mg/cm^2	Oxide phases[a]
B-1900	900	2/3	$NiMoO_4$(s), NiO(m), spinel ($a_o = 8.15\times10^{-10}$ m)(m), tapiolite (w)
		3	$NiMoO_4$(vs), NiO(vs), spinel ($a_o = 8.15\times10^{-10}$ m)(m), tapiolite (w)
	1000	2/3	$NiMoO_4$(w), spinel ($a_o = 8.15\times10^{-10}$ m)(vw), tapiolite(vw), α-Al_2O_3(vvw)
		3	$NiMoO_4$(w), spinel ($a_o = 8.15\times10^{-10}$ m)(vvw)
VIA	900	[b]2/3	NiO(s), $NiMoO_4$(m), spinel ($a_o = 8.15\times10^{-10}$ m)(m), tapiolite(w)
		3	NiO(vvs), $NiMoO_4$(m), spinel ($a_o = 8.15\times10^{-10}$ m)(w), tapiolite(w)
	1000	2/3	Spinel ($a_o = 8.15\times10^{-10}$ m)(vs), tapiolite(vs), NiO(m), $NiMoO_4$(m)
		3	$NiMoO_4$(m), tapiolite(m), spinel ($a_o = 8.15\times10^{-10}$ m)(w), NiO(w)
713C	900	2/3	$NiMoO_4$(m), spinel ($a_o = 8.20\times10^{-10}$ m)(w), tapiolite (w), NiO(w), Cr_2O_3(vvw)
		3	$NiMoO_4$(s), spinel ($a_o = 8.20\times10^{-10}$ m)(w), NiO(w), tapiolite(vw), Cr_2O_3(vvw)
	1000	2/3	$NiMoO_4$(w), NiO(w), spinel ($a_o = 8.20\times10^{-10}$ m)(w), Cr_2O_3(vw)
		3	NiO(m), $NiMoO_4$(m), spinel ($a_o = 8.20\times10^{-10}$ m)(w), tapiolite(vvw)
738	900	2/3	$NiMoO_4$(m), NiO(m), spinel ($a_o = 8.30\times10^{-10}$ m)(m), tapiolite(vw)
		[c]3	NiO(s), $NiMoO_4$(m), spinel ($a_o = 8.30\times10^{-10}$ m)(w), tapiolite(vw), α-Al_2O_3(vvw)
	1000	2/3	Cr_2O_3(w), spinel ($a_o = 8.30\times10^{-10}$ m)(w), TiO_2(w), NiO(vw), $NiMoO_4$(vw)
		3	Cr_2O_3(w), spinel ($a_o = 8.30\times10^{-10}$ m)(w), TiO_2(w), NiO(w), $NiMoO_4$(vw)

[a]Listed in order of decreasing intensity of diffraction pattern.
Symbols indicate a qualitative measure of diffraction pattern intensity, which is a function not only of oxide composition but also of oxide thickness: v = very, s = strong, m = medium, w = weak.

[b]Several samples that resisted hot corrosion showed $NaTaO_3$(vs), spinel ($a_o = 8.15\times10^{-10}$ m)(s), tapiolite(m), NiO(w).

[c]Sample that was preoxidized and resisted hot corrosion, showed NiO(vs), $NaTaO_3$(s), spinel ($a_o = 8.30\times10^{-10}$ m)(m).

TABLE III. - PHASES IDENTIFIED BY X-RAY DIFFRACTION IN PEELED OXIDE SCALES FORMED AFTER Na_2SO_4-INDUCED OXIDATION IN 1 ATMOSPHERE OF FLOWING OXYGEN

Alloy	Temperature, °C	Dosage of Na_2SO_4, mg/cm^2	Oxide phases[a]
B-1900	900	2/3	NiO(vs), $NiMoO_4$(w), spinel ($a_o = 8.15\times10^{-10}$ m)(w), tapiolite(w)
		3	NiO(vs), $NiMoO_4$(m), spinel ($a_o = 8.15\times10^{-10}$ m)(m), tapiolite(m)
	1000	2/3	NiO(vs), $NiMoO_4$(m), spinel ($a_o = 8.15\times10^{-10}$ m)(m), tapiolite(w)
		3	NiO(vs), $NiMoO_4$(m), spinel ($a_o = 8.15\times10^{-10}$ m)(m), tapiolite(m)
VIA	900	2/3	NiO(vs), spinel ($a_o = 8.15\times10^{-10}$ m)(m), tapiolite(vw)
		3	NiO(vs), spinel ($a_o = 8.15\times10^{-10}$ m)(w), tapiolite(vw), $NiMoO_4$(vvw)
	1000	2/3	NiO(vs), spinel ($a_o = 8.15\times10^{-10}$ m)(s), tapiolite (s), $NiMoO_4$(m)
		3	NiO(s), tapiolite(w), spinel ($a_o = 8.15\times10^{-10}$ m)(w)
713C	900	2/3	NiO(s), spinel ($a_o = 8.20\times10^{-10}$ m)(m), tapiolite (w), $NiMoO_4$(vw)
		3	NiO(s), spinel ($a_o = 8.20\times10^{-10}$ m)(m), tapiolite (w), $NiMoO_4$(vw)
	1000	2/3	NiO(vs), $NiMoO_4$(s), spinel ($a_o = 8.20\times10^{-10}$ m)(m), tapiolite(w)
		3	NiO(s), spinel ($a_o = 8.20\times10^{-10}$ m)(m)
738	900	2/3	NiO(vs), spinel ($a_o = 8.30\times10^{-10}$ m)(m)
		3	NiO(vs), spinel ($a_o = 8.30\times10^{-10}$ m)(m), $NiMoO_4$(vw)
	1000	2/3	NiO(vs), spinel ($a_o = 8.30\times10^{-10}$ m)(m)
		3	NiO(vs), spinel ($a_o = 8.30\times10^{-10}$ m)(m)

[a]Listed in order of decreasing intensity of diffraction pattern.
Symbols indicate a qualitative measure of diffraction pattern intensity, which is a function not only of oxide composition but also of oxide thickness: v = very, s = strong, m = medium, w = weak.

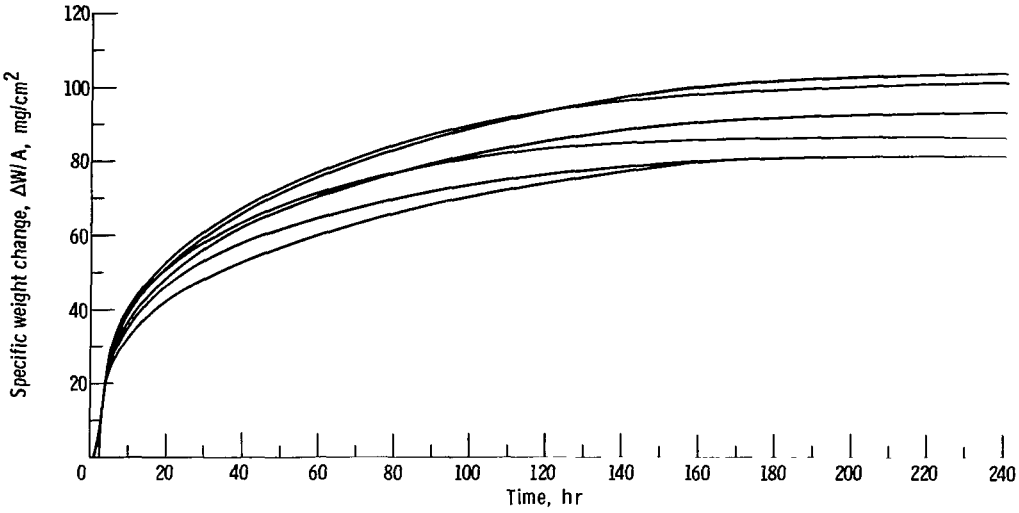

Figure 1. - Rate of hot corrosion of six B-1900 specimens at 900° C in 1 atmosphere of slowly flowing oxygen. Dosage, 2/3 milligram per square centimeter of Na_2SO_4.

Figure 2. - Typical specimen that exhibited accelerated oxidation: alloy B-1900; dosage, 2/3 milligrams per square centimeter of Na_2SO_4; oxidized for 140 hours at 900° C in slowly flowing oxygen and cooled to room temperature.

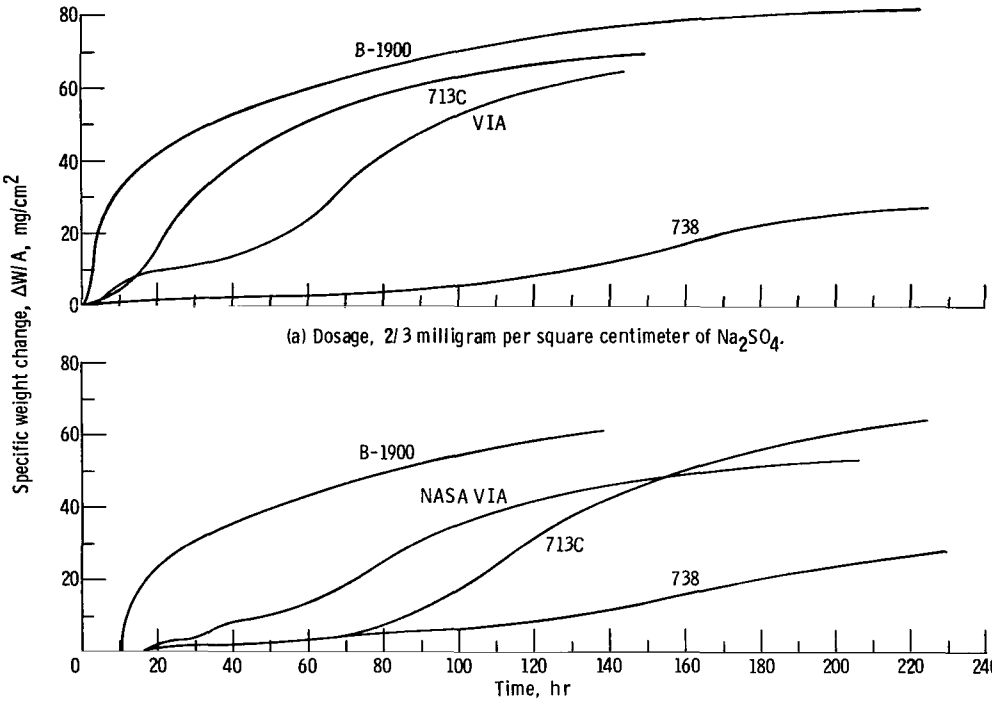

(a) Dosage, 2/3 milligram per square centimeter of Na_2SO_4.

(b) Dosage, 2/3 milligram per square centimeter of Na_2SO_4. Specimens preoxidized 100 hours at 900° C.

Figure 3. - Rate of hot corrosion of alloys at 900° C in slowly flowing oxygen.

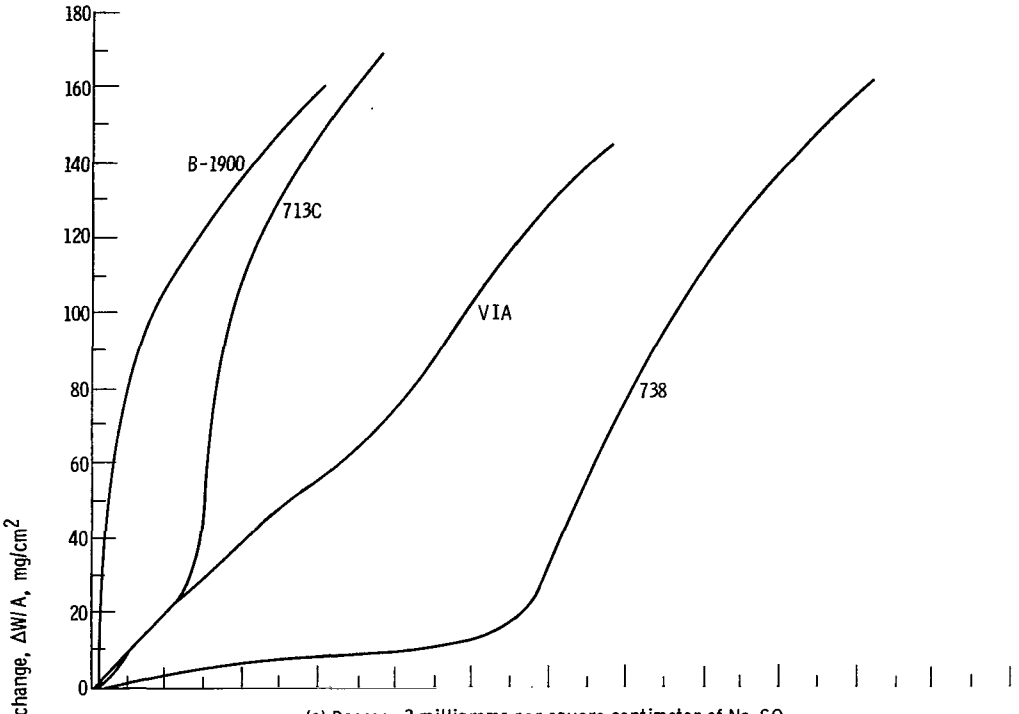

(c) Dosage, 3 milligrams per square centimeter of Na_2SO_4.

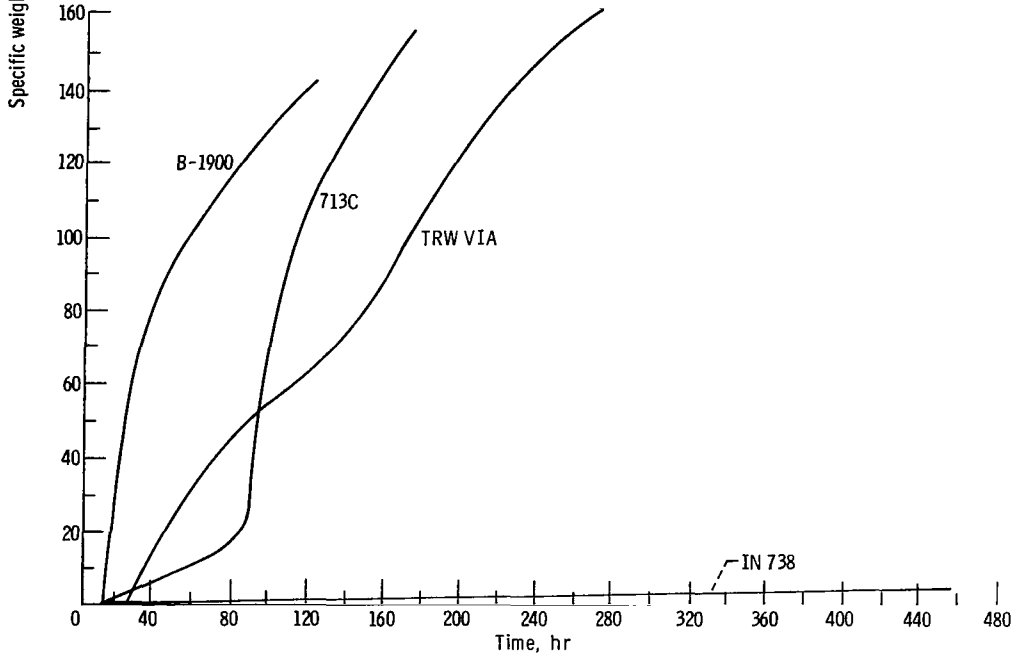

(d) Dosage, 3 milligrams per square centimeter of Na_2SO_4. Specimens preoxidized 100 hours at 900° C.

Figure 3. - Concluded.

Figure 4. - Specimen of 738 that exhibited slightly accelerated oxidation. Dosage, 2/3 milligram per square centimeter Na_2SO_4; oxidized for 220 hours at 900° C in slowly flowing oxygen and cooled to room temperature.

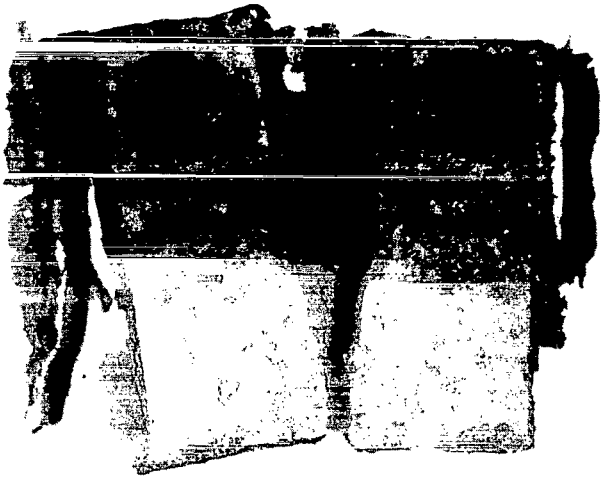

Figure 5. - Specimen of 738 that exhibited catastrophic oxidation. Dosage, 3 milligrams per square centimeter of Na_2SO_4; oxidized for 400 hours at 900° C in slowly flowing oxygen and cooled to room temperature.

Figure 6. - Specimen of 738 that exhibited resistance to hot corrosion. Preoxidized for 100 hours at 900° C in slowly flowing oxygen; coated with 3 milligrams per square centimeter of Na_2SO_4 and oxidized for 460 hours at 900° C in slowly flowing oxygen.

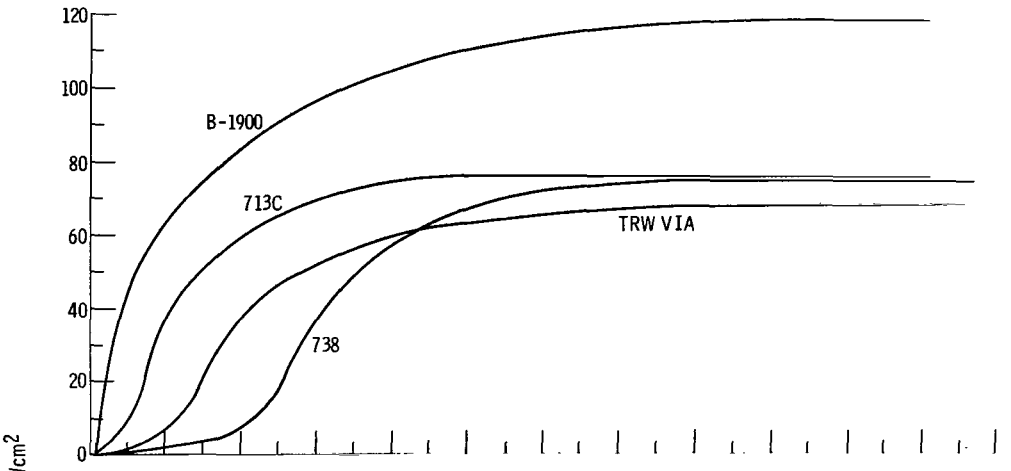

(a) Dosage, 2/3 milligram per square centimeter of Na_2SO_4.

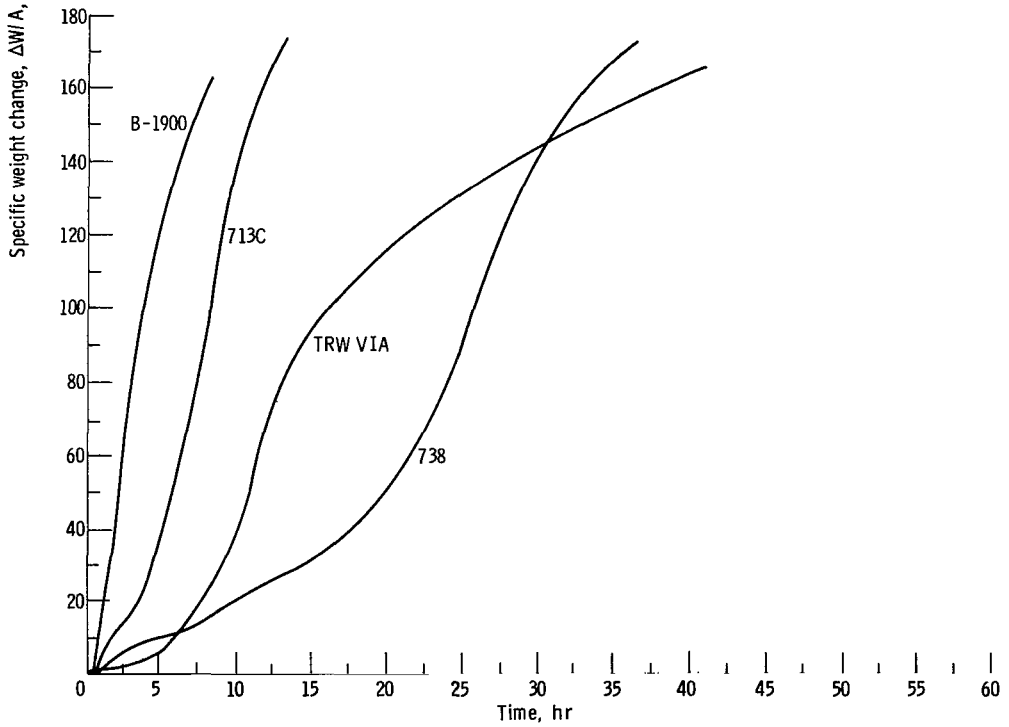

(b) Dosage, 3 milligrams per square centimeter of Na_2SO_4.

Figure 7. - Rate of hot corrosion of alloys at 1000^0 C in slowly flowing oxygen.

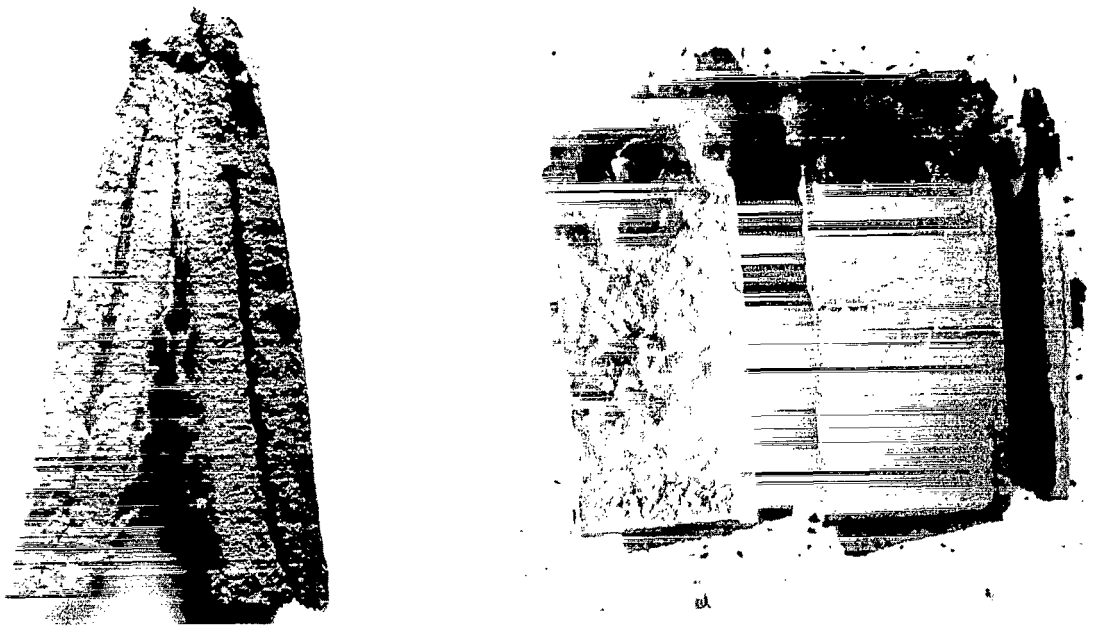

(a) Edge-on view.

(b) Side view of intact oxide scales after removal from platinum hook.

Figure 8. - Typical specimen that exhibited catastrophic oxidation: alloy VI A; dosage, 3 milligrams per square centimeter; oxidized 40 hours at 1000° C in slowly flowing oxygen and cooled to room temperature.

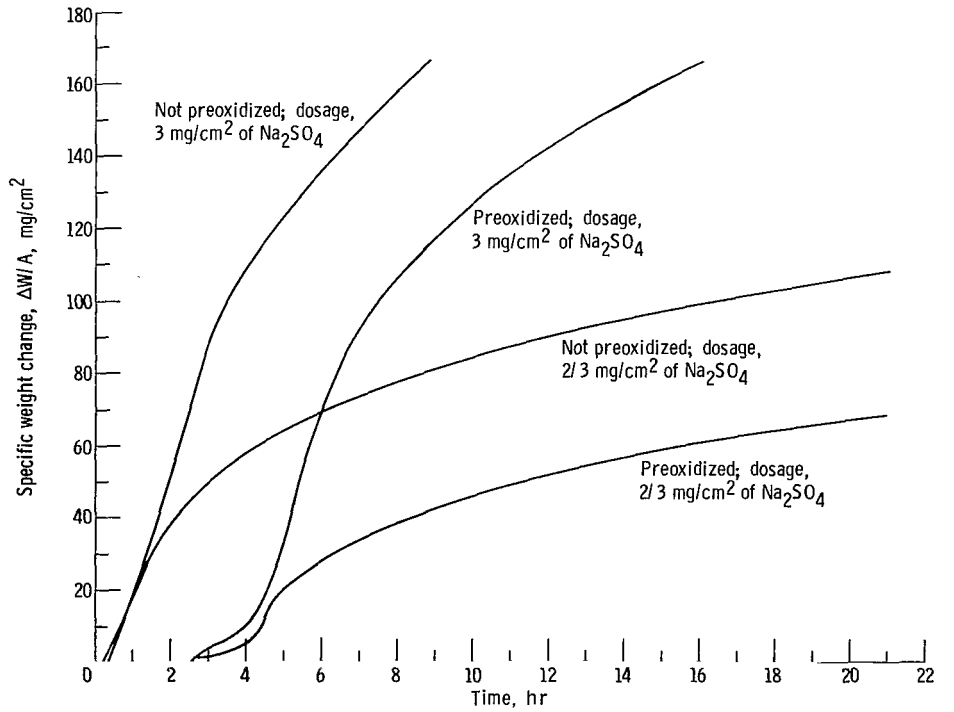

Figure 9. - Rate of hot corrosion of B-1900 at 1000° C in slowly flowing oxygen; effect of preoxidation of specimens for 100 hours at 1000° C.

NATIONAL AERONAUTICS AND SPACE ADMINISTRATION
WASHINGTON, D.C. 20546

OFFICIAL BUSINESS
PENALTY FOR PRIVATE USE $300

SPECIAL FOURTH-CLASS RATE
BOOK

POSTAGE AND FEES PAID
NATIONAL AERONAUTICS AND
SPACE ADMINISTRATION
451

U.S.MAIL

"The aeronautical and space activities of the United States shall be conducted so as to contribute . . . to the expansion of human knowledge of phenomena in the atmosphere and space. The Administration shall provide for the widest practicable and appropriate dissemination of information concerning its activities and the results thereof."

—NATIONAL AERONAUTICS AND SPACE ACT OF 1958

NASA SCIENTIFIC AND TECHNICAL PUBLICATIONS

TECHNICAL REPORTS: Scientific and technical information considered important, complete, and a lasting contribution to existing knowledge.

TECHNICAL NOTES: Information less broad in scope but nevertheless of importance as a contribution to existing knowledge.

TECHNICAL MEMORANDUMS: Information receiving limited distribution because of preliminary data, security classification, or other reasons. Also includes conference proceedings with either limited or unlimited distribution.

CONTRACTOR REPORTS: Scientific and technical information generated under a NASA contract or grant and considered an important contribution to existing knowledge.

TECHNICAL TRANSLATIONS: Information published in a foreign language considered to merit NASA distribution in English.

SPECIAL PUBLICATIONS: Information derived from or of value to NASA activities. Publications include final reports of major projects, monographs, data compilations, handbooks, sourcebooks, and special bibliographies.

TECHNOLOGY UTILIZATION PUBLICATIONS: Information on technology used by NASA that may be of particular interest in commercial and other non-aerospace applications. Publications include Tech Briefs, Technology Utilization Reports and Technology Surveys.

Details on the availability of these publications may be obtained from:

SCIENTIFIC AND TECHNICAL INFORMATION OFFICE

NATIONAL AERONAUTICS AND SPACE ADMINISTRATION

Washington, D.C. 20546